THE ASTROPHYSICAL JOURNAL, 519:354–371, 1999 July 1

CONSTRAINTS ON THE EVOLUTION OF MASSIVE STARS THROUGH SPECTRAL ANALYSIS. I. THE WC5 STAR HD 165763

D. JOHN HILLIER
Department of Physics and Astronomy, University of Pittsburgh, Pittsburgh, PA 15260
AND
D. L. MILLER
Steward Observatory, University of Arizona, Tucson, AZ 85721
Received 1998 May 29; accepted 1999 February 3

ABSTRACT

Using a significantly revised non-LTE radiative transfer code that allows for the effects of line blanketing by He, C, O, Si, and Fe, we have performed a detailed analysis of the Galactic Wolf-Rayet (W-R) star HD 165763 (WR 111, WC5). Standard W-R models consistently overestimate the strength of the electron scattering wings, especially on strong lines, so we have considered models where the wind is both homogeneous and clumped. The deduced stellar parameters for HD 165763 are as follows:

$$L = 2.0 \times 10^5\ L_\odot\ ,\quad R_* = 1.8\ R_\odot\ ,\quad \dot{M} = 1.5 \times 10^{-5}\ M_\odot\ \mathrm{yr}^{-1}\ ,\quad V_\infty = 2300\ \mathrm{km\ s}^{-1}\ ,$$

$$N(\mathrm{C})/N(\mathrm{He}) = 0.4\ ,\quad X(\mathrm{C}) = 0.462\ ,\quad N(\mathrm{O})/N(\mathrm{He}) = 0.1\ ,\quad X(\mathrm{O}) = 0.154\ .$$

The above results are for a clumped model in which the volume filling factor of the clumps is assumed to be 0.1 and implies (assumes) a distance of 1.55 kpc for HD 165763. Similar results are obtained for homogeneous models except that the deduced mass loss is larger, approximately $5.0 \times 10^{-5}\ M_\odot\ \mathrm{yr}^{-1}$. The clumped model gives consistently better agreement with the line profiles, particularly the red wings, confirming the scenario that W-R winds are clumped. Because of the severe blending in WC stars and the simplicity of our approach, it is not feasible to deduce the actual filling factor or mass-loss rate. The quantity that can be determined from line strengths using our models is $\dot{M}/f^{1/2}$. Using the evolutionary models of Maeder and Meynet, we find that the stellar abundances and parameters are consistent with a star of initial mass 60 $M_\odot$ and that has a present mass 10 $M_\odot$.

The stellar parameters deduced for HD 165763 are significantly different from earlier analyses. The deduced luminosity is a factor of 2 larger, and a smaller core radius is found. The smaller radius is in better agreement with expectations from stellar evolution calculations. Both of these changes can be attributed to the effects of line blanketing. The deduced C/He abundance is similar to earlier calculations, and the O/He abundance had not previously been determined.

The observed iron spectrum, principally due to Fe V and Fe VI, is well reproduced using a solar iron mass fraction, although a variation of at least a factor of 2 about this value cannot be precluded. In particular, the models naturally produce the Fe V emission feature centered on 1470 Å and the complex Fe emission/absorption spectrum at shorter wavelengths. Also, Fe strongly modifies the line strengths and profile shapes shortward of 1800 Å and must be taken into account if we are to successfully model this region.

The reddening toward HD 165763 does not follow the mean Galactic extinction law. We determine the reddening law toward HD 165763 by comparing our model continuum levels to observations. In order to simultaneously match the UV, optical, and particularly the infrared fluxes, we used the parameterized reddening law of Cardelli, Clayton, and Mathis with $E_{B-V} = 0.3$ and $R = 4.5$, where $R = A_V/E_{B-V}$.

Based on both observational and theoretical suggestions we have considered models in which the wind is still accelerating at large radii. In particular, we discuss models in which the velocity law can be characterized by $\beta = 1$ for $r < 10R_*$ but that undergo a substantial velocity increase (~ 600 km s^{-1}) beyond $10R_*$. These models appear to give slightly better fits to the line profiles, but the improvements are small, and it is difficult to gauge whether observational data require such a velocity law.

We cannot yet determine whether the winds of W-R stars are driven by radiation pressure, because we neglect many higher levels of iron in our model ions, and we do not include important elements such as cobalt and nickel. However, the "wind problem" in W-R stars is less severe than previously assumed if clumping occurs. For our clumped model, the single scattering limit is only exceeded by a factor of 10 compared to 3 times this value for a homogeneous wind. Clumping appears to be the key to explaining the apparent high mass-loss rates determined for W-R stars and is extremely important in understanding how or even whether W-R winds are driven by radiation pressure. A reduction in W-R mass-loss rates has important implications for stellar evolution calculations.

Subject headings: stars: abundances — stars: fundamental parameters — stars: individual (HD 165763) — stars: Wolf-Rayet

1. INTRODUCTION

Wolf-Rayet (W-R) stars of the carbon sequence (WC) show incredibly complex spectra. Their spectra are dominated by emission lines that are generally so densely packed that the continuum is masked from view. With new modeling techniques we are now able to reproduce the spectra of WC stars over UV, optical, and IR wave bands, allowing considerable improvement in quantitative spectroscopic analysis. In this paper we discuss our analysis of the Galactic WC5 star HD 165763 (WR 111). Previous theoretical investigations of this star (e.g., Hillier 1989; Koesterke & Hamann 1995) were restricted to modeling individual lines and neglected line blanketing. Here we use new sophisticated non-LTE line blanketed atmosphere models discussed by Hillier & Miller (1998).

HD 165763 is relatively bright ($v = 8.23$; Massey 1984), has only a moderate reddening ($E_{B-V} = 0.3$; § 3), and is presumed to be single, since it shows no absorption lines and no radial velocity variations (Lamontagne 1983). The star is linearly polarized, but the polarization is small ($\approx 0.3\%$) and constant, indicating that it is probably interstellar in origin (St.-Louis et al. 1987). Spectropolarimetric observations show that there is no line effect (i.e., the polarization across an emission line is constant), confirming that the polarization is of interstellar origin and strongly suggesting that the star is spherically symmetric (Kurosawa, Hillier, & Schulte-Ladbeck 1998). All of these attributes make HD 165763 an ideal candidate for spectroscopic analysis. One drawback of this star is the high velocity of the wind ($V_\infty \sim 2300$ km s^{-1}), which causes extensive line blending and hinders line identification.

This work is the first part of a larger project to analyze a sequence of WC stars covering the full range of spectral types. The principal goal of our investigation is to better determine the fundamental parameters and abundances of the WC stars in order to provide more stringent constraints for evolutionary models of these massive stars. In this paper we will discuss the prototypical WC5 star HD 165763. Because the analysis presented in this paper is the first to utilize models of WC stars with full line blanketing due to He, C, O, and Fe treated in a self consistent manner, we provide a more thorough discussion of the analysis and theoretical models than will be presented in subsequent papers.

The paper is organized as follows: In § 2 we discuss the observational data we use for comparison with the models, and in §§ 3 and 4, respectively, the reddening and distance of HD 165763 are discussed; § 5 describes the three models used in this paper. In § 6 we describe our implementation of clumping, and in § 7 we compare our three models. The ionization structure is discussed in § 8. In §§ 9 and 10 we discuss specific features due to iron and silicon, and in § 11 the effect of a slightly different velocity law is discussed. In § 12 the radio fluxes determined from our model are compared to measured values; abundances are discussed in § 13, and the wind momentum problem is discussed in § 14. A discussion of our results is given in § 15.

2. OBSERVATIONAL DATA

The models we calculate can predict the spectrum at all wavelengths from the far UV to the near-infrared. In order to analyze the plausibility of our models, good quality flux-calibrated data are required. For the *IUE* range we have used the high-resolution spectrum of I. D. Howarth (1990, private communication). This spectrum has been created from several *IUE* spectra and has a good signal-to-noise ratio of 30:1 in most spectral regions. The flux calibration of these observations should be revised using the new *IUE* calibration, but this is beyond the scope of the present paper and will be less important than the uncertainties in the reddening law (see § 3).

For the optical region we have used the low-resolution spectrophotometry of Massey (1984). These data are of only moderate quality for HD 165763, but it is the only flux-calibrated data available. These data have been augmented by data from the atlas of Smith & Kuhi (1982, private communication; WC Atlas) and by our own high-resolution optical observations.

Near-infrared spectra and a tabulation of equivalent widths (EWs) for the strongest lines have been given by Conti, Massey, & Vreux (1990), and infrared magnitudes (1–4 μm) have been tabulated for HD 165763 by Eenens & Williams (1992). Eenens & Williams also provide corrections to these magnitudes due to the influence of emission lines. Unfortunately, longer wavelength flux information is sparse and of uncertain quality. The 10 μm measurement of 0.25 Jy by Abbott, Telesco, & Wolff (1989, private communication) is substantially smaller than the determinations of Cohen, Kuhi, & Barlow (1975) of 0.41 Jy and a more recent *IRAS* measurement of 0.79 Jy at 12 μm by Cohen (1995; see § 12). Cohen (1995) also provides a 25 μm measurement of 0.47 Jy for HD 165763, whereas a 6 cm radio flux of 0.33 ± 0.1 mJy is given by Bieging, Abbott, & Churchwell (1982).

Infrared spectra published by Eenens, Williams, & Wade (1991) have also been utilized, but unfortunately these data are not flux calibrated. P. A. Crowther (1997, private communication) has also kindly supplied moderate-resolution ($R = 600$–1000) IR spectra taken at United Kingdom Infrared Telescope (UKIRT) in 1994 August. These flux-calibrated spectra were scaled slightly so their continua matched the measured IR fluxes of Eenens & Williams (1992).

Generally, the data from different sources are in good agreement. For example, the *IUE* and optical ranges show moderate agreement around the atmospheric cutoff. In addition to the discrepancy in the 10 μm flux noted earlier, there is also an inconsistency in the literature regarding the strength of the important transition He I λ10830, the only UV, optical, and near-IR He I line that is not severely blended. Values in the literature fall into two groups, those that give an EW of approximately 100 Å (Kuhi 1968; Howarth & Schmutz 1992) and those that give an EW around 180 Å (Schmutz, Hamann, & Wessolowski 1989; Vreux, Andrillet, & Biemont 1990). Our own observations and those of P. A. Crowther (1997, private communication) indicate a value closer to the latter, and it is this value that has been used for our analysis. We believe the discrepancy is probably observational and does not indicate actual variations in the He I λ10830 flux. In particular, because of the rapid decline in CCD sensitivity longward of 10000 Å and the limited wavelength coverage longward of 10830, it is very difficult to locate the continuum. New IR spectra (Eenens et al. 1991; P. A. Crowther 1997, private communication) clearly show that there is emission redward of He I λ10830, emission that is not seen in the Howarth & Schmutz (1992) spectrum of HD 165763.

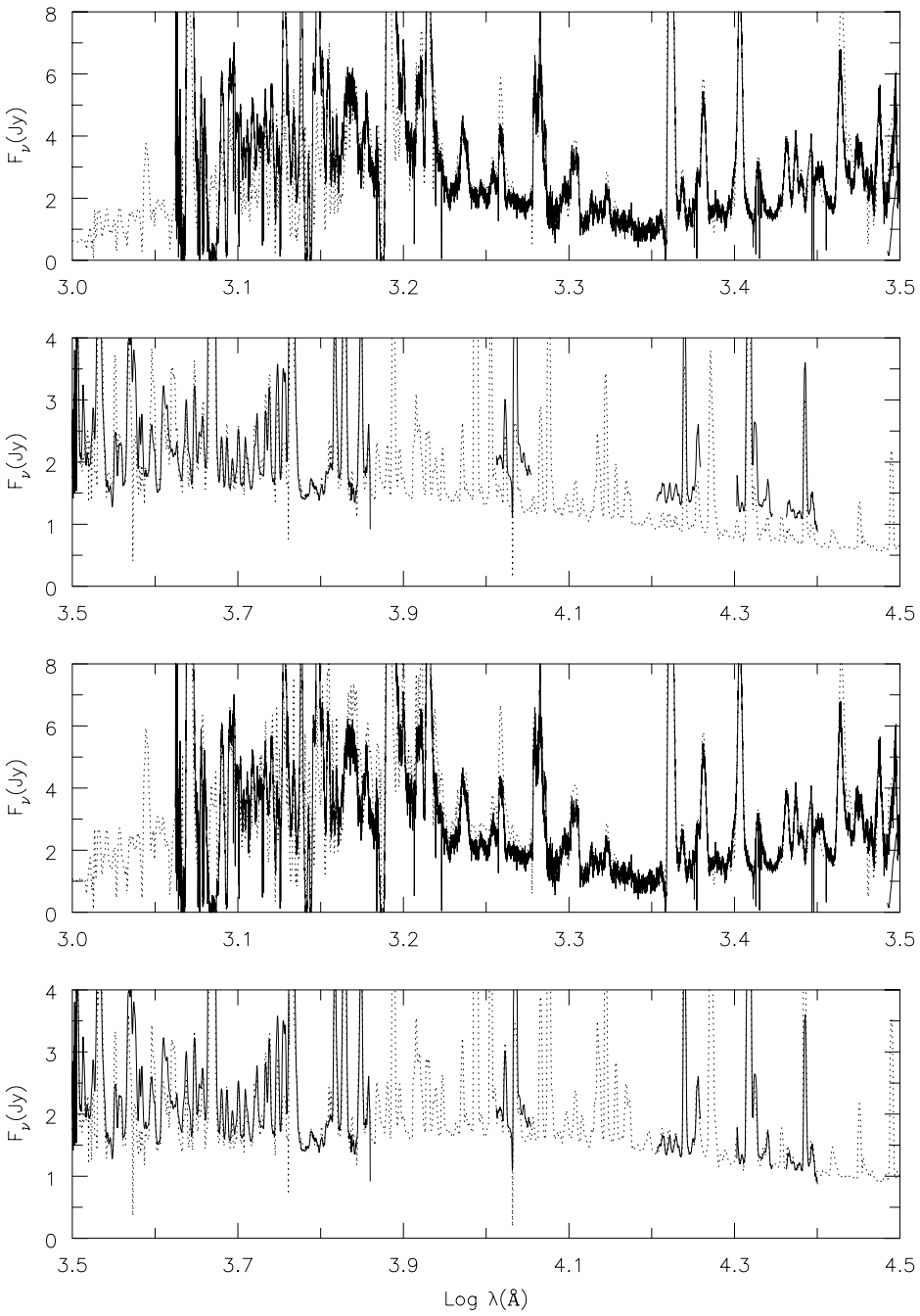

FIG. 1.—Comparison between the observed energy distribution (*solid line*) and that of the final model. In the top two panels the model spectrum has been reddened using a normal reddening law with $R = 3.1$ and $E_{B-V} = 0.24$ at a distance of 1.95 kpc. Note the flux deficiency of the model in the UV (log $\lambda < 3.2$) and the extreme flux deficiency in the IR (log $\lambda > 4.0$). In the lower two panels the model has been reddened using $R = 4.5$ and $E_{B-V} = 0.30$ at a distance of 1.55 kpc. Now there is good agreement between the theoretical and observed continuum at all wavelengths.

In order to facilitate the comparison over UV, optical, and IR spectral regions all wavelengths are plotted for vacuum.

3. REDDENING

HD 165763 has been the subject of several interstellar reddening studies. These studies typically find an E_{B-V} of around 0.3 (e.g., 0.26 by Nussbaumer et al. 1982; 0.34 by Morris et al. 1993). However, as noted by Morris et al. (1993), HD 165763 lies in a region where the interstellar reddening properties are different from the Galactic average (Meyer & Savage 1981). Consequently, all such determinations must be regarded with caution.

In an extensive study of interstellar extinction laws, Cardelli, Clayton, & Mathis (1988) showed that the shape of the interstellar extinction law can generally be described by a single parameter R ($R = A_V/E_{B-V}$, where A_V is the extinction at 5560 Å). In order to allow for a nonstandard extinction law (i.e., $R \neq 3.1$), we have adopted their formulation for the interstellar extinction.

TABLE 1

SUMMARY OF MODEL ATOMS

	Model A		Model B		Model C		
Species	N_S	N_F	N_S	N_F	N_S	N_F	n(max) of C
He I	27	39	...	...	...	...	14
He II	13	30	...	...	...	...	30
He III.....	1	1	...	...	...	...	...
C II	3	3	22	22	...	...	5
C III	44	70	78	138	99	243	30
C IV	45	50	...	...	59	64	30
C V	1	1	...	...	...	...	...
O II.....	3	3	...	...	...	...	2
O III	25	25	...	...	...	...	3
O IV	10	10	53	72	...	...	4
O V	34	34	75	152	...	...	7
O VI.....	13	13	25	31	...	...	8
O VII	1	1	...	...	...	...	...
Si IV	37	37	37	48	...	...	10
Si V	1	1	...	...	...	...	...
Fe IV	21	280	...	...	...	...	...
Fe V	19	182	...	...	...	...	...
Fe VI	10	80	...	...	57	439	...
Fe VII	14	153	...	...	...	...	...
Fe VIII.....	1	1	...	...	...	...	...

NOTE.—Only modified atoms are listed for models B and C.

At wavelengths greater than 1500 Å, the extinction law of Cardelli et al. (1988) for $R = 3.1$ is very similar to Seaton (1979), but it departs significantly at shorter wavelengths. In preliminary work on HD 165763, Hillier & Miller (1998) found that the Seaton law tended to better reproduce the UV fluxes, although there were still inconsistencies.

In the early part of this study we concentrated on matching the UV and optical spectra only. With the inclusion of 1–3 μm IR photometry it was found that the IR continuum was severely underestimated (Fig. 1). This problem plagued both clumped and unclumped models of HD 165763. The only way to remove this discrepancy was to adopt a nonstandard R value of 4.5, which gave a good fit from 1200 Å to 10 μm.[1] Whereas problems in fitting the UV continuum shortward of 1500 Å indicated a possible problem with the standard extinction law, it was the disparity of the model and observed IR fluxes that provided the strongest evidence for a peculiar extinction law. Crowther et al. (1995b) found that the WN7 star HD 93162 (WR 25) also showed a peculiar extinction law ($R = 4.6$), and, similarly, it was the difficulty matching the observed UV/optical and IR fluxes simultaneously that provided the strongest evidence for a peculiar extinction. Both these cases indicate that it is necessary to use UV, optical, and IR fluxes to determine reddening parameters for W-R stars.

An independent determination of R could be made from broadband polarimetric observations, if they were available. The value of R is known to be correlated with the wavelength at which the interstellar polarization (ISP) is a maximum (Serkowski, Mathewson, & Ford 1975; Clayton & Mathis 1988).

[1] The model flux agrees with the 10 μm flux measurement of D. C. Abbott et al. (1989, private communication) but not with the higher values of Cohen (Cohen et al. 1975; Cohen 1995). The larger values are inconsistent with the model.

4. DISTANCE

HD 165763 is thought to be a member of the Sgr OB1 association (Lundstrom & Stenholm 1984) with a distance of 1.6 ± 0.4 kpc. However, because of problems with the interstellar extinction toward this cluster, this distance estimate may need revision. Thus, in our modeling of HD 165763, we chose to reproduce the continuum fluxes for a nominal distance of 1.6 kpc, but because of the complex dependence of the fluxes on the stellar parameters, abundances, clumping parameters, and interstellar extinction (which has to be determined from the fitting procedure), we chose not to fine-tune the parameters to reproduce the observed fluxes for a distance of exactly 1.6 kpc. Hence, for each model, we indicate the distance that would be required if the model and continuum fluxes were to agree.

Our results can be converted to other distances using the following formulae:

$$\dot{M}_{\rm new} = \dot{M}_{\rm old}\left(\frac{d_{\rm new}}{d_{\rm old}}\right)^{1.5}, \quad (1)$$

$$R_{*\rm new} = R_{*\rm old}\left(\frac{d_{\rm new}}{d_{\rm old}}\right), \quad (2)$$

$$T_{\rm eff,new} = T_{\rm eff,old}, \quad (3)$$

$$L_{\rm new} = L_{\rm old}\left(\frac{d_{\rm new}}{d_{\rm old}}\right)^{2}. \quad (4)$$

The velocity law and abundances should remain the same. The above scaling was found by Schmutz et al. (1989) to describe WN stars and is based on the premise that models with the same transformed radius [$\propto R_*(V_\infty/\dot{M})^{2/3}$], $T_{\rm eff}$, and composition show very similar spectra. It was also found to hold, at least approximately, for WC stars by Hamann et al. (1992); however, the exact relations for WC

stars may differ slightly from those above because of the complex nature of their atmospheres. Najarro, Hillier, & Stahl (1997) found similar relations for the luminous blue variable (LBV) P Cygni.

5. THE MODEL

To perform a spectroscopic analysis of HD 165763 we used the improved non-LTE line-blanketing code of Hillier & Miller (1998), which allows for line blanketing, most importantly, in the iron-line–dominated ultraviolet and fully allows for the effects of line overlap.

This paper is based on a series of calculations that have been undertaken using atomic models of varying complexity. A summary of the atomic levels for three classes of models is presented in Table 1, where N_S is the number of super levels, and N_F is the number of full levels. Also given in the table is the principal quantum number of the highest energy level for non–iron group elements. In our calculations we only solve for the populations of the superlevels. The populations of individual levels that make up a superlevel are found by assuming that all levels in the superlevel have the same departure coefficient (see Hillier & Miller 1998 for a full description of the model and our implementation of superlevels).

Model "A" was used as the "workhorse" for the initial investigation. Stellar parameters and abundances were adjusted to obtain optimal agreement with observed continuum levels and line strengths. The overall fit of model A was good with the exception of several oxygen and carbon lines (see § 7). Model "B" was utilized in an attempt to better fit these lines. In the B models the number of atomic levels in the C II–III, O IV–VI, and Si IV model ions were substantially increased. A final refinement was made by again increasing the number of levels in the C III and C IV atomic models and using an improved Fe IV atom based on the work of Butler (1995a), Kurucz (1993), and the Opacity Project (Seaton et al. 1987). In this final model, "C," the C III ion was extended to include levels up to $n = 30$ in order to match IR C III recombination lines. This model was also found to enhance the strength of some optical C III lines. Similarly, to improve the fit of recombination lines between high levels of C IV, the C IV atom was extended from $n = 16$ to $n = 30$. This change was also found to increase the strength of C IV λ5471 [n(10)–n(7)], so that the optimal C/He abundance ratio was reduced from 0.6 to 0.4.

Our calculations include a frequency range from 59 Å to 20 mm, which encompasses over 99% of the flux. In order to minimize computational effort, most models were computed with only 40 depth points; detailed tests showed that this is more than adequate for the parameter range of interest. The final models were computed with 60 depth points.

6. CLUMPING

Evidence for clumping in W-R winds comes from several sources that include profile variability (e.g., Robert 1994) and time-dependent calculations of line-driven winds (Owocki, Castor, & Rybicki 1988). In addition, Hillier (1991b) invoked clumping to explain why the strengths of the electron scattering wings were overestimated by standard spectra calculations. Schmutz (1997) has performed more detailed calculations of the influence of clumping on the wind dynamics and the line profiles in the WN5 star HD 50896 and was able to obtain excellent profile fits. Discussion of the evidence for clumping in W-R winds and the difficulties incorporating it into stellar models can be found in Hillier (1997). A discussion of the consequences of clumping in hot-star winds is given by Moffat (1994), and an extensive discussion of variability and structures in hot-star winds can be found in the workshop devoted to these topics (Moffat et al. 1994).

As briefly discussed by Hillier (1997), we have adopted a simple filling factor approach to include clumping in our models. We assume that the winds of the W-R star are clumped with a volume filling factor, f, and that there is no interclump medium. This approach is similar to that of Abbott, Bieging, & Churchwell (1981), who allowed for the effects of clumping on mass-loss rates derived from radio fluxes, and to that of Schmutz (1997), who utilized a filling factor approach in his investigation of HD 50896. The filling factor technique has been adopted over our earlier approach (Hillier 1991b), because it is computationally much faster. In particular, we can use a spatial grid of 40–60 depth points with a filling factor approach compared to 194 depth points for our previous study.

We parameterize our filling factor according to

$$f(r) = a + (1 - a) \exp\left[-v(r)/b\right], \tag{5}$$

where the parameter a describes the density contrast and b the location in the wind at which clumping becomes important. The latter reflects the fact that radiation instabilities are not expected to be important in the inner part of the wind (Owocki 1991). Thus our simple formula gives the desired result that f approaches unity as v goes to zero and approaches a as v becomes large. With our definition of the filling factor, the density in any clump is given by

$$\rho(r) = \frac{\dot{M}}{4\pi r^2 v(r) f(r)}, \tag{6}$$

whereas the average density at any location is simply $f(r)\rho(r)$. A more complicated formulation could also have been adopted, but our simple formulation (eq. [5]) gives qualitatively good results.

To solve the transfer equation we assume that the clumps are small compared to the mean free path of the photons. This assumption is reasonable for continuum processes but breaks down for line photons, because the clumps are expected to have a size larger than the Sobolev length (Puls, Owocki, & Fullerton 1993). The effect of this assumption has not been examined but should not dramatically alter the conclusions we draw from our models. The adopted procedure, for example, conserves photons and yields the correct strength of optically thin recombination lines.

In this formulation of clumping, the expressions for the opacities and emissivities are

$$[\eta(r), \chi(r)]_{\rm clump} = [\eta(r), \chi(r)] f(r), \tag{7}$$

where η and χ are computed using populations and densities appropriate to the clumps. The solution of the radiative transfer equation and the equilibrium equations then proceeds exactly as in the unclumped model.

The clumped and unclumped spectra are qualitatively very similar. Observationally, it would be difficult to distinguish between the two spectra on the basis of line strengths and continuum shape. The main difference is seen in line profiles. In the clumped model the profiles are nar-

rower, the strength of the red electron scattering wing is reduced, and line blending is more easily discerned (see Fig. 2). These effects simply reflect the reduction in electron scattering optical depth. Comparison with observation indicates that the clumped profiles are generally in better agreement with the observations. This confirms earlier suggestions (e.g., Hillier 1991b) that the electron scattering wings in current W-R models are overestimated. Whereas we can conclude f, (i.e., a) is less than 1 for HD 165763, we have not attempted to derive its value, because of the severe line blending in WC stars, uncertainties in the velocity law, and the relative insensitivity of the profiles to f. In the fitting procedure $\dot{M}$ and f are highly correlated: the quantity $\dot{M}/f^{1/2}$ is determined by the spectroscopic modeling. The same quantity ($\dot{M}/f^{1/2}$) is derived from the observed radio fluxes (Abbott et al. 1981). In WN stars the less severe line blending should allow constraints to be placed on the clumping factor.

With the exception of $\dot{M}$, the stellar parameters and abundances do not change significantly with the inclusion of clumping. In some sense this result just reflects the fact that the clumping in our models is fairly uniform through the line-forming region. We could enhance the He I λ10830 line, for example, by specifically enhancing the clumping in its formation region ($r > 10R_*$). This, however, may necessitate a higher luminosity. Theoretical guidance to the nature of the clumps and their radial dependence is needed if we are to realistically include clumping in our wind models.

It should be stressed that the clumped model *must* have a lower mass-loss rate than the homogeneous model. Without a reduction in $\dot{M}$, the predicted spectrum is qualitatively different and of much lower excitation. Further, we would like to remind the reader that the aim of this work is not to derive clumping parameters. Rather, it is to provide an estimate of uncertainties in the derived parameters due to clumping and, as discussed earlier, to yield profiles more consistent with observation by reducing the electron scattering optical depth.

Whereas several groups (e.g., Lamers & Waters 1984; Nugis 1994; Blomme & Runacres 1997) have considered the influence of clumping on the IR energy distribution of O stars, much less effort has been devoted to the very difficult problem of computing full non-LTE spectra (i.e., lines and continua) from a clumped and structured wind. Detailed preliminary calculations have been performed by Puls et al. (1993) for the formation of resonance lines in O star winds. In those calculations the nonmonotonicity of the velocity law was taken into account. They show that the shape of both the absorption and emission component of a classic P Cygni profile can be significantly affected by a clumped and structured wind.

7. COMPARISON OF MODELS

Our final model for HD 165763 has the following parameters:

$$L = 2.0 \times 10^5\ L_\odot\ ,\quad R_* = 1.8\ R_\odot\ ,$$
$$\dot{M} = 1.5 \times 10^{-5}\ M_\odot\ \mathrm{yr}^{-1}\ ,$$
$$\dot{M}/f^{1/2} = 4.7 \times 10^{-5}\ M_\odot\ \mathrm{yr}^{-1}\ ,$$
$$V_\infty = 2300\ \mathrm{km\ s}^{-1}\ ,\quad d = 1.55\ \mathrm{kpc}\ ,$$
$$a = 0.1\ ,\quad b = 200\ \mathrm{km\ s}^{-1}\ ,$$
$$N(\mathrm{C})/N(\mathrm{He}) = 0.4\ ,\quad X(\mathrm{C}) = 0.462\ ,$$
$$N(\mathrm{O})/N(\mathrm{He}) = 0.1\ ,\quad X(\mathrm{O}) = 0.154\ ,$$
$$E_{B-V} = 0.3\ ,\quad R = 4.5\ .$$

The value of the luminosity is a factor of 2 higher than found in earlier studies, and the core radius is smaller. As noted earlier, $\dot{M}$ and f are not independent: the quantity $\dot{M}/f^{1/2}$ is derived from the fitting procedure.

The model spectrum, from 1150 Å to 2.5 μm, is compared with observation in Figure 3. The model has been reddened according to the interstellar extinction law of Cardelli et al. (1988). The two reddening parameters and the stellar distance were chosen to give agreement between the model fluxes and those observed at all wavelengths. No other scaling was performed. Our final model includes clumping, since it generally provides better fits to observed line profiles, particularly on the red side. With the exception of these scattering wings, the homogeneous models produce qualitatively similar fits.

Overall, there is excellent agreement between the model and observed spectra. Many line fluxes agree to within 10%. In particular, notice the excellent fit to the observed data between 2350 and 3000 Å. With the scale of the plot, it is difficult to see the difference between the observed and model data in this region.

A perfect fit is not possible, and thus a quality judgment was exercised to choose the final adopted model. Models with a lower luminosity (e.g., $L = 1.5 \times 10^5$) increase the strength of C III lines, but fits to C IV $\lambda\lambda$1550 and 5805 are noticeably worse, as are the fits for oxygen lines arising from

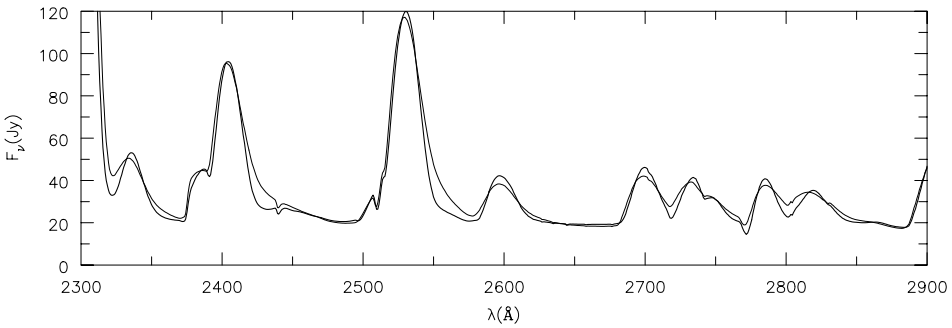

FIG. 2.—Figure illustrating the effects of clumping on line profiles. The heavy line shows the spectrum of a clumped model with $f = 0.1$ (i.e., $a = 0.1$), and the light line shows that of an unclumped model. With the exception of the mass-loss rate, the parameters of the models are identical. Notice the reduction in the strength of the electron scattering wings and the cleaner separation between partially overlapping emission lines. The strength of the electron scattering wings depend on both how and where the lines are formed in the atmosphere (Hillier 1991b).

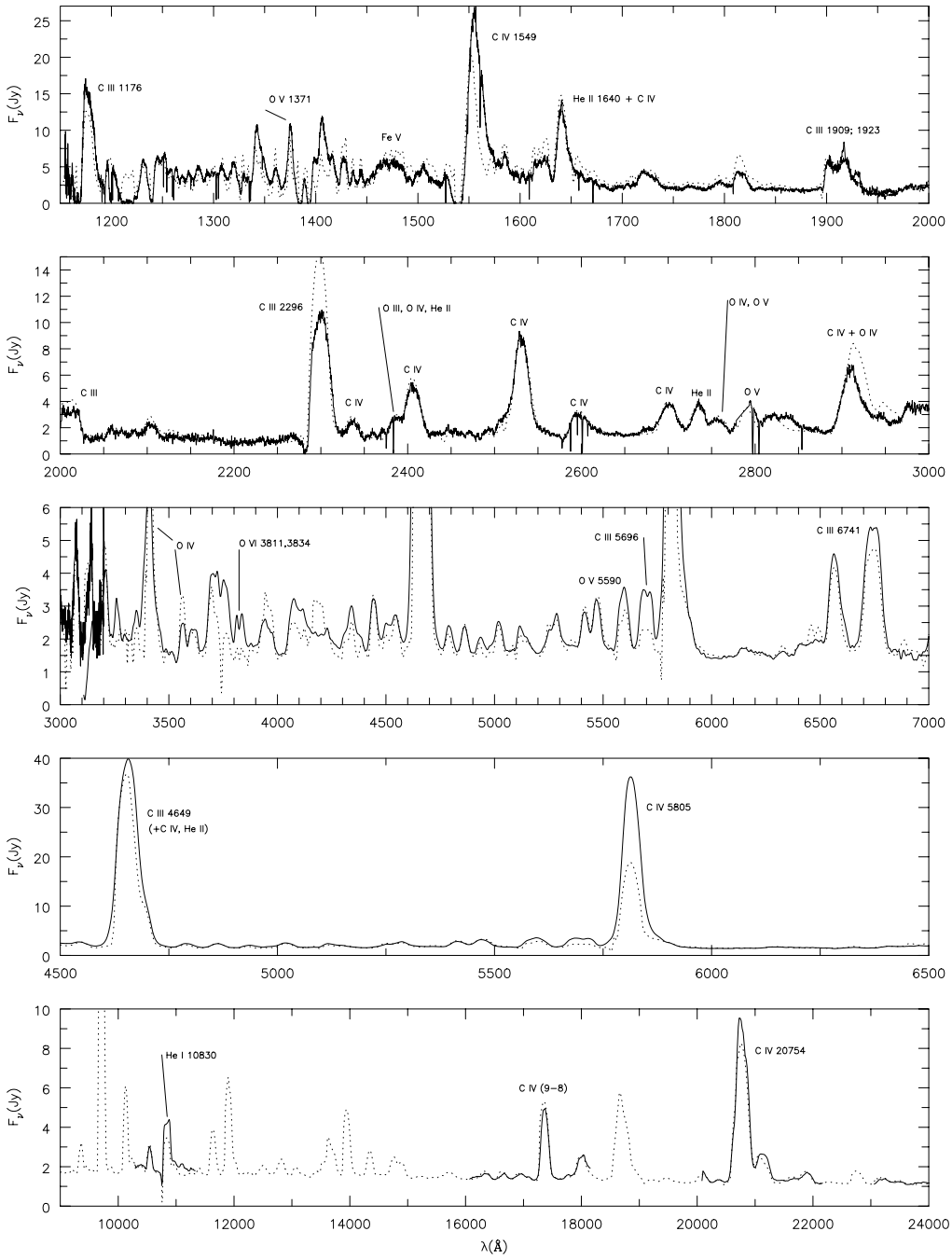

FIG. 3.—Comparison of the final model "C" (*dotted line*) with observations. The model spectrum has been reddened and scaled (by adjusting the distance) to match the observations. There is generally excellent agreement between the spectra, with a few important discrepancies such as the O VI $\lambda\lambda$3811, 3834 complex.

high-ionization species (e.g., O VI, O V). On the other hand, models with a higher luminosity (e.g., $L = 3 \times 10^5$), while providing a much better estimate for the strength of both C IV $\lambda\lambda$1550 and 5805, strongly underestimate by factors of 4 or more the C III lines such as $\lambda\lambda$5696, 6740, and 9700.

Although line strengths are in general agreement, there are noticeable discrepancies. There are several possible reasons for this, but we do not believe they invalidate the model. First, improvements to the model atoms are needed. For example, the oscillator strengths for C III are excellent, but the photoionization data needs to be improved. Second, many of the model iron ions are still rather simple, and additional levels must be included. This and the addition of more species will improve the blanketing calculations and should help overcome some of the discrepancies in the UV. It is worth noting that every advance in wind calculations by ourselves and others has led to a significant improvement in the quality of the model fits.

To highlight the difficulty of predicting some line strengths, consider C III λ5696. This line was discussed by Hillier (1989), who indicated that, because the upper level of this transition has an alternate decay route, the line strength is very model sensitive. For a model similar to that discussed above ($L = 1.7 \times 10^5\ L_\odot$, C/He = 0.6) we examined the effect of a factor of 4 increase in the Fe abundance, with all other parameters fixed. As expected, there was a strong

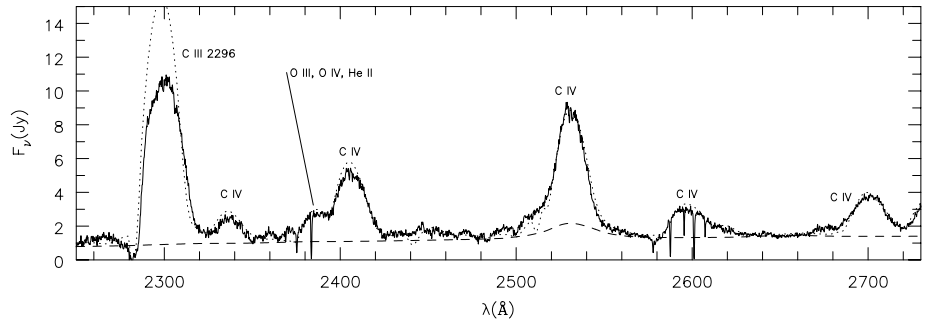

FIG. 4.—High-resolution plot to illustrate the fit quality of several UV lines. The dashed line is the continuum—the bump near 2530 Å is a resonance in a photoionization cross section. The principal lines in this region are C III λ2286, C IV λ2326 (8–5, high *l*), O III λ2390, and several transitions belonging to the C IV (5–4) array (λλ2404, 2530, 2595). The overall agreement between individual line profiles is excellent, although the strength of C III λ2296 is clearly overestimated.

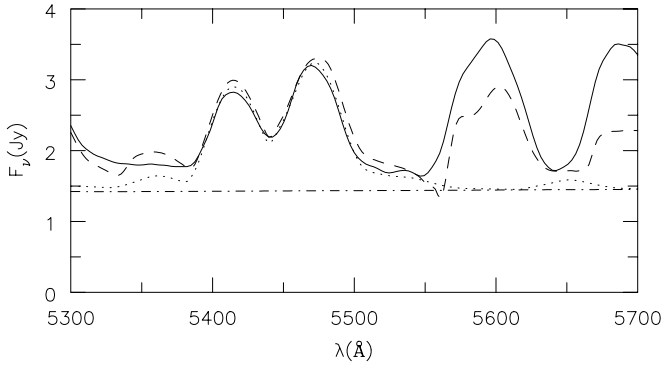

FIG. 5.—High-resolution plot of the region around the He II λ5411/C IV λ5471 complex. The solid line shows the observed data, the dashed line is the model spectrum, and the dotted line shows the direct contribution to the model spectrum by He II and C IV emission lines only. The model continuum is also shown. Notice that the profile of the He II/C IV complex is in excellent agreement with observation, although this is somewhat dependent on the continuum normalization. The excess broadening in the C IV λ5471 line in the full model spectrum may be due to other lines in this region, possibly O III.

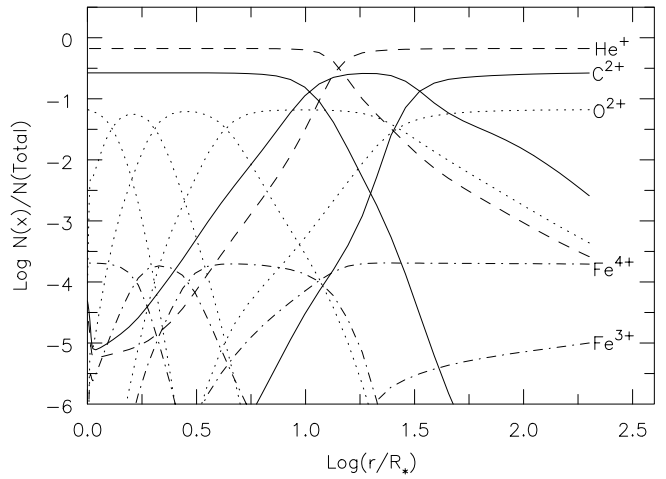

FIG. 6.—Plot of the ionization fraction, $N(X)/N$(total ionic population), as a function of radius for He, C, O, and Fe. The normalization of each species simply reflects the relative abundances. The highest ionization stages at depth are He^{2+}, C^{4+}, O^{6+}, and Fe^{7+}. The important characteristic to notice is the rapid decline in the ionization with radius.

enhancement of Fe emission and absorption in the UV, particularly between 1400 and 2000 Å. Longward of 2000 Å, the enhanced iron abundance generally had little influence except for C III λ5696, which increased in strength by more than a factor of 2. Interestingly, some other C III lines (e.g., λ6740) actually decreased slightly in strength. For a higher luminosity model ($L = 2.0 \times 10^5\ L_\odot$) the changes in C III λ5696 were not as dramatic. C III λ8500 was also found to be sensitive to the Fe abundance, changing by a factor of 2 in both luminosity models for changes of a factor of 4 in the Fe abundance.

To illustrate the agreement in profile shapes, two regions are shown at higher resolution in Figures 4 and 5. As can be seen, there is good agreement between model and observed line profiles. Better fits might be obtained by fine-tuning the velocity, but such an exercise would not yield any useful information. Instead, there are several improvements that need to be made to the calculations including additional atomic species, additional atomic levels, improved atomic data, and a more realistic treatment of the highly structured nature of radiation driven winds.

The He II λ5411/C IV λ5471 complex (Fig. 5) is often used to determine the C/He abundance ratio. A casual comparison between model and observations would suggest that the model is overestimating the line width of the C IV λ5471 line. A more thorough analysis reveals that the line is broader because of a significant contribution from an O III line. This is illustrated in Figure 5, where we have plotted the model results allowing for He II and C IV emission only. Although these lines are generally regarded as "blend-free," it is apparent that other lines must contribute to the spectrum in this region. In this model *we allow for the contribution of 93 lines between 5350 and 5550* Å. Whereas most of the lines are very weak, some do contribute. The good fit to the peaks of the λ5411/λ5471 complex is based on forcing agreement between the observed and model continuum fluxes at 6000 Å. Data at shorter wavelengths (e.g., 4500–5500 Å) suggest a slightly different (<10%) normalization might be more appropriate. In order to analyze the spectra of WC stars adequately it is necessary to have high-quality spectrophotometry.

7.1. *Infrared Spectral Region*

Initial comparisons of our theoretical spectra (using atomic models "A" and "B") with the infrared spectra of

Eenens et al. (1991) and P. A. Crowther (1997, private communication) showed qualitative agreement with the observations, although the C III recombination lines were predicted to be much too weak. This simply reflected our adopted atomic model for C III, which only included levels with $n \leq 10$.

To improve agreement in the IR we extended our model C III atom to include all $2snl$ levels up to $n = 30$. States with $l \geq 7$, $n \leq 14$, and the same principal quantum number and parity were treated as single states, although they were combined into superlevels when solving the statistical equilibrium equations, whereas all l states for a given principal quantum number and parity for $n > 14$ were combined into a single level. Hydrogenic cross sections were generally adopted, although oscillator strengths to low-lying levels were scaled so that the progression along a series was smooth. The resulting C III atom for model "C" had a total of 243 levels grouped into 99 superlevels.

With the new C III model atom, the C III recombination lines are significantly stronger and are in reasonable agreement with observation. Importantly, the extended atom has also increased the strength of some C III lines in the UV and optical. In particular, there has been a significant increase in the strength of C III $\lambda\lambda$5696, 6742, 9700 and the C III complex between 4000 and 4300 Å. This illustrates one of the difficulties in modeling C III lines in early WC stars; many atomic levels must be included in order to accurately predict line strengths. The same is true for many other ions.

8. IONIZATION STRUCTURE

The typical ionization structure for a model of HD 165763 is shown in Figure 6. As is readily apparent from the figure, the ionization state of the gas declines rapidly with radius. In the inner regions of the wind the dominant ionization states are He^{2+}, C^{4+}, O^{6+}, and Fe^{7+}, whereas in the outer regions He^{+}, C^{2+}, O^{2+}, and Fe^{4+}/Fe^{3+} are dominant. The declining ionization structure results from several factors, including the large optical depth of the wind shortward of 228 Å, the proximity of several ionization edges to 228 Å, and the decreasing importance of ionizations from excited states in the outer wind. The excellent agreement of our theoretical spectra with the observational data, from UV to near-IR wavelengths, indicates that the ionization structure of our model is qualitatively similar to the actual structure in the wind of HD 165763.

Work by Schulte-Ladbeck, Eenens, & Davis (1995) previously showed that in HD 165763 the high-ionization lines tend to be systematically narrower than the emission lines originating from lower ionization species. There is considerable scatter in their plot (Fig. 7), which is not surprising given the different line formation processes, optical depth effects, and the enormous problems of line blending. This trend is easily explained by an ionization structure of the type shown in Figure 6; i.e., the higher ionization lines are formed deeper in the wind where the outflow velocity is smaller. We find that the general form of the ionization structure in our models does not change with the clumping factor for our simple implementation, provided we adjust the mass-loss rate so that the spectrum of HD 165763 is reproduced.

9. THE IRON CONTINUUM

The importance of iron in the spectra of W-R stars has been known for over a decade. Using crude spectral synthesis techniques Nugis & Sapar (1985) demonstrated that the high-resolution spectrum of HD 192163 between 1245 and 1720 Å was dominated by overlapping emission and P Cygni lines of Fe V and Fe VI. Koenigsberger (1990a) used laboratory Fe intensities to estimate line intensities and showed that Fe V and Fe VI emission was particularly important below 1500 Å in HD 193077 (WR 138, WN + abs). By comparison with WN stars, Hillier (1991a) showed that Fe emission is also important in WC stars.

Work by several groups (e.g., Koenigsberger & Auer 1985; Eaton, Cherepaschuk, & Khaliullin 1985a, 1985b) has also shown that iron absorption provides an important wind opacity source in WN + O binary systems. An excellent illustration of the influence of Fe V and Fe VI in the UV region of the WNE + O binary V444 Cygni is given by Koenigsberger (1990b).

The spectrum of HD 165763 shortward of 1500 Å is a rich and complex blend of predominately iron lines. To demonstrate the importance of Fe, we calculate an emergent spectrum with and without iron lines included (Fig. 7). The impact is obvious: Fe blanketing is extremely important in the spectrum formation region 1000–1500 Å and dominates shortward of 500 Å.

The importance of both emission and absorption processes in producing the Fe spectrum can be demonstrated observationally by comparing two WC stars of similar spectral type but with different terminal velocities. For example, a comparison of the spectrum of HD 165763 with the LMC star HD 32402 (WC4; Torres, Conti, & Massey 1986) in Figure 8 shows that the shape and position of features

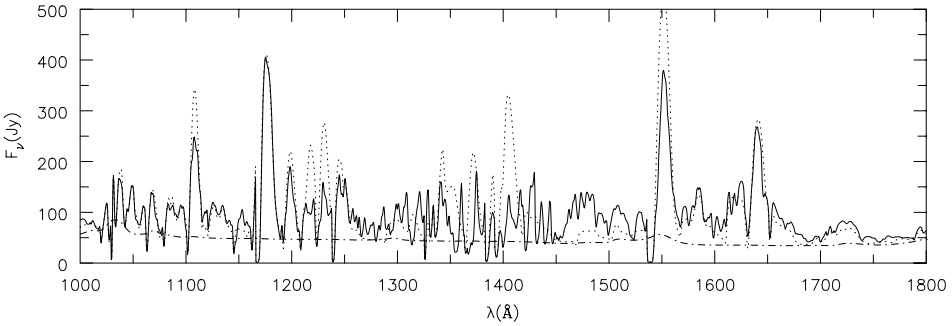

FIG. 7.—Plot showing the influence of iron on the theoretical spectrum between 1000 and 1800 Å. The solid line is the full theoretical spectrum, the dotted line is the theoretical spectrum computed with no iron lines included, and the dot-dashed line is the model continuum. Fe lines contribute significantly to both the emission and absorption in this spectral region, and, specifically, the C IV $\lambda\lambda$1548, 1551 resonance doublet is weakened. The emission/absorption lines are so closely packed that the continuum level in this spectral region is masked and can best be determined via theoretical modeling.

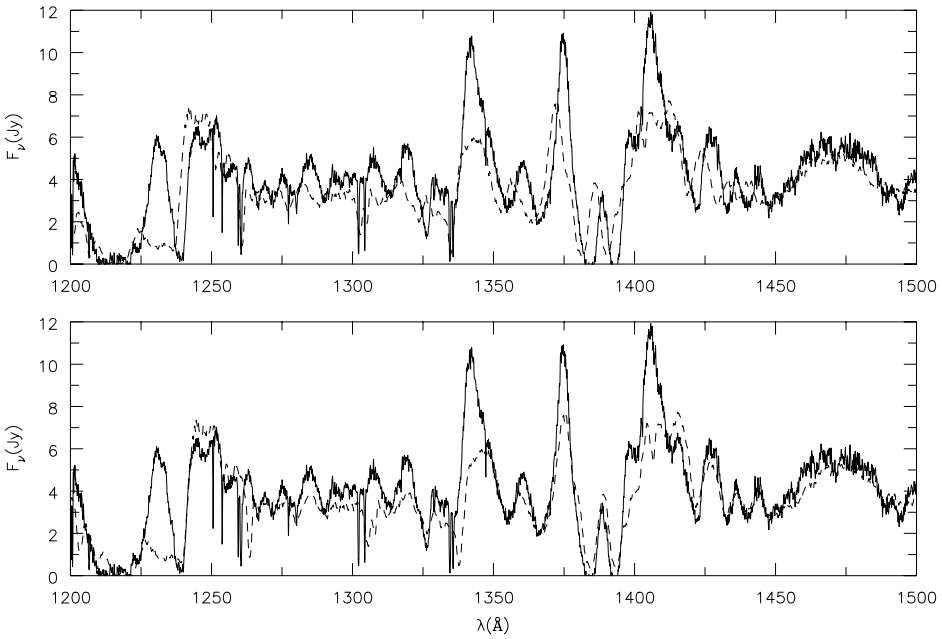

FIG. 8.—Comparison of the spectrum of HD 165763 (WC5, $V_\infty = 2300$ km s^{-1}; *solid curve*) with the LMC star HD 32402 (WC4, $V_\infty = 2900$ km s^{-1}; Gräfner et al. 1998). The continuum level of HD 32402 has been scaled to match that of HD 165763. In the top figure, the spectrum of HD 32402 has been corrected for an assumed radial velocity of 150 km s^{-1}. As can be seen, many of the features in the two spectra are in different locations. In the bottom figure, the rest-frame spectrum of HD 32402 has been redshifted by 650 km s^{-1}. Notice the excellent correspondence between many of the apparent absorption and emission features. The similarity of the shift to the difference in the terminal velocities indicates the importance of wind absorption in the spectra of WC stars, which is primarily Fe absorption in this spectral region.

around 1420–1450 Å are strongly determined by absorption processes, and do not represent pure emission lines.

As apparent from Figures 1, 3, and 9, the spectrum between 1150 (the *IUE* cutoff) and 1800 Å is in reasonable agreement with our final model. In particular, there is good correspondence between emission and absorption features, and with the broad Fe V emission bump between 1450 and 1500 Å. It is evident that Fe absorption has severely modified the profiles of several emission features in this spectral region. The major discrepancy between our model and observation occurs around the Si IV/O IV complex near 1400 Å (Fig. 9). Here the Fe absorption is too strong and has eaten away much of the Si IV emission (§ 10).

Iron absorption can also have a drastic effect on emission lines of other species. For some lines, the emission is completely eaten away, whereas in other cases the emission profile is severely modified. This explains why the O V λ1371, the O V analog to C III λ2296, has its maximum near 1375 Å rather than at its laboratory wavelength of 1371.3 Å. Interestingly, we see that the C IV resonance doublet at 1548, 1551 Å can also be influenced by iron absorption, although there is little observational evidence for such absorption in HD 165763. The emission peak of the C IV resonance transition is also significantly offset from its laboratory wavelength. Hillier (1989) suggested that because of the large optical depth of this line, its full Voigt profile should be considered in order to obtain a better fit.

Given the uncertainties in the reddening correction shortward of 1500 Å, the continuum level is surprisingly accurate. But these uncertainties in the interstellar extinction law make the study of the iron spectrum shortward of 1500 Å difficult. Clearly, what is needed is the actual interstellar extinction law toward HD 165763, which could perhaps be found from studies of nearby stars. Alternatively, as the

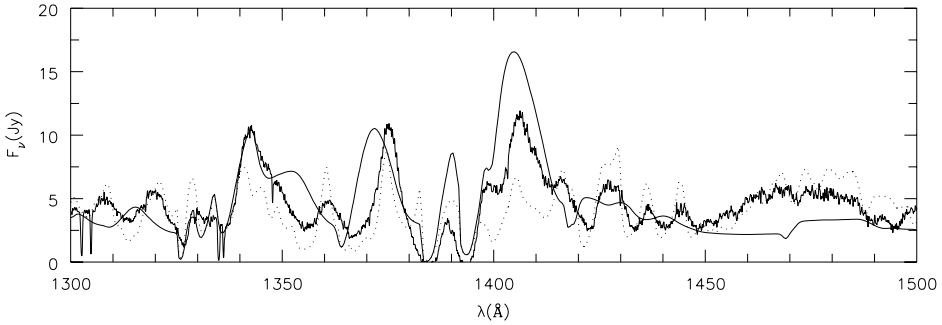

FIG. 9.—Spectrum of HD 165763 in the neighborhood of the Si IV $\lambda\lambda$1392, 1403 resonance doublet. The full synthetic spectrum (*dotted line*) provides a poor match to the complex emission feature near 1400 Å but does provide a good fit, at least qualitatively, to the rest of the spectrum. The thin solid line shows the theoretical spectrum when iron lines are neglected. Comparison of this spectrum with the full synthetic spectrum reveals how the O V λ1371 line and the Si IV doublet have been distorted by Fe absorption. Clearly, the poor fit to the Si IV doublet is due to excess Fe absorption, primarily Fe V.

models become more sophisticated we should be able to use the C III λ1175 line to constrain the interstellar extinction in the UV. However, based on the predictions for other C III lines we must allow for the possibility of a factor of 2 error in the predicted strength of this line, and thus we cannot presently make a reliable estimate of the interstellar UV extinction.

The observed region shortward of 1600 Å is very complex and will require further detailed analysis. Present models tend to produce too much absorption compared to the Fe emission. This may be attributable to the lack of upper levels in our model Fe ions. Currently we include only the $3d^n$, $3d^{(n-1)}4s$ and the $3d^{(n-1)}4p$ configurations. The inclusion of these higher levels will also provide an additional driving force for the wind.

10. SILICON FEATURES

Several silicon lines have been identified in the spectra of WC stars by Smith & Kuhi (1982, private communication; W. C. Atlas) and Nussbaumer et al. (1982). Our models for HD 165763 show some silicon lines; however, those due to Si III are predicted to be weak, and, unfortunately, none of the Si IV lines predicted are blend-free.

The strongest Si IV lines expected in the spectrum of HD 165763 are the Si IV doublets $\lambda\lambda$1392, 1403; $\lambda\lambda$1722, 1727; and $\lambda\lambda$4089, 4116. The first of these is the well-known resonance transition, and, although present in HD 165763, its strength is difficult to estimate because of the presence of iron absorption and overlapping O IV emission. Just shortward of the *IUE* cutoff, our models predict that Si IV $\lambda\lambda$1122, 1128 should be seen.

Models with a solar silicon abundance, by mass, unfortunately do not provide a good fit to the observed spectrum around the Si IV resonance doublet at 1400 Å. The disparity is most probably due to problems with the numerous Fe lines in this spectral region. In fact, as can be gleaned from Figure 9, Fe absorption has completely eaten away this Si IV emission. Although such absorption is seen in the spectrum of HD 165763, it is not as strong as we predict. This complex blending in the neighborhood of the silicon resonance line is the reason why observers in the past have struggled to separate the relative contributions of Si IV and O IV. The problem of iron absorption from 1300 to 1500 Å making line analysis difficult is not unique to WC stars: Koenigsberger (1990b) found Fe absorption in this region to be very important in the WNE-O binaries they studied.

The other two silicon doublets, $\lambda\lambda$1722, 1727 and $\lambda\lambda$4089, 4116, arise from the same upper level. This level could be populated through recombination or through continuum fluorescence via a UV transition connected to the ground state at 458 Å. Assuming the transitions are optically thin, we find that if Si IV $\lambda\lambda$1722, 1727 is the dominant contributor to the feature near 1725 Å, Si IV will also be an important contributor to the feature near 4100 Å. However, both of these features could arise from other sources.

The feature at 1725 Å can be identified with Fe IV; however, Fe IV is not very prevalent in WC5 spectra (although it is clearly present in WC6 and WN6 spectra). Generally, when the model excitation is such as to produce the 1725 Å feature, we overpredict the strength of other Fe IV emission lines between 1600 and 1800 Å. The complex emission feature near 4100 Å has a significant C III contribution. Because the predicted strength of the C III line has an uncertainty of up to a factor of 2, the exact contribution to this feature is unknown but could approach 100%. Thus it is not clear how much silicon contributes to the spectrum of HD 165763 and to WC5 stars in general.

11. VELOCITY LAW

In most previous analyses of W-R stars it has been usual to adopt a $\beta = 1$ velocity law. However, model fits are not sensitive to the β exponent because of the large breadth of their emission lines. Indeed, Hillier (1991c) showed that fits using $\beta = 1$ and $\beta = 3$ for a WN5 star were virtually identical.

In the usual β-velocity law, the exponent β determines the velocity law at all depths, with the largest acceleration occurring at large depths and very little in the outer layers. However, observational work on binaries by Koenigsberger (1990b) suggested that the wind was still accelerating at 14 $R_\odot$. Further work by Auer & Koenigsberger (1994) investigating the structure of W-R winds using binaries supports this conclusion. Theoretical work by Gayley, Owocki, & Cranmer (1995) and Springman (1994) also suggests that significant acceleration occurs at large radii. Thus a simple β-velocity law may not be an accurate description of the velocity field in W-R stars.

To overcome this limitation of a single parameter specifying the shape of the velocity law over most of the atmosphere, we have augmented the normal β-velocity law with a second β-velocity component. The adopted velocity law has the form

$$v(r) = \frac{V_0 + (V_\infty - V_{\rm ext} - V_0)(1 - R_*/r)^{\beta_1} + V_{\rm ext}(1 - R_*/r)^{\beta_2}}{(1 + V_0/V_{\rm core}) \exp\,[(r - R_*)/h_{\rm eff}]} . \quad (8)$$

As discussed by Najarro et al. (1997), the denominator in the above equation allows a hydrostatic density structure to be obtained at depth; $V_{\rm ext}$ and β_2 are the parameters that allow the velocity law in the outer parts of the wind to be specified separately from the inner region. Figure 10 shows the classic β-velocity law and our new velocity law, in which there is a very slow extended acceleration.

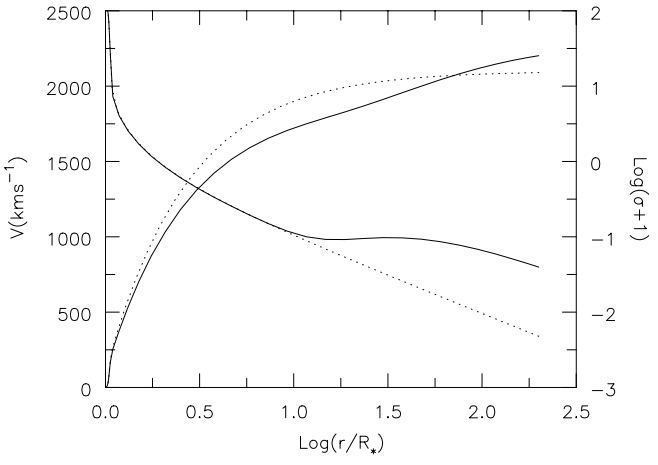

FIG. 10.—Comparison between the classic $\beta = 1$ velocity law (V_∞ = 2100 km s^{-1}; *dotted curves*) and that used in our final model (V_∞ = 2300 km s^{-1}, $V_{\rm ext}$ = 400 km s^{-1}, $\beta_1 = 1$, $\beta_2 = 50$; *solid curves*). With the latter velocity law, the wind is still accelerating beyond 30R_*. This enhanced acceleration in the outer layers is indicated by the larger value of $\sigma + 1$, which is a measure of the velocity gradient ($\sigma + 1 = d \ln v / d \ln r$). The parameters of the velocity laws were chosen to give similar emission line profiles.

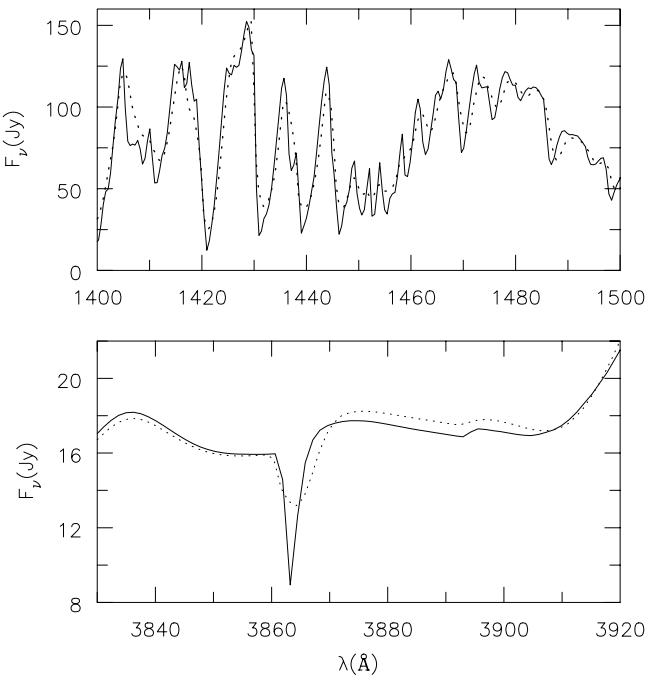

FIG. 11.—Two spectral regions contrasting the different profiles for a normal β-velocity law (*dotted lines*) and a "slower" velocity law with extended acceleration. In the top panel it can be seen that the Fe absorption components are weaker and smoother with the slower velocity law. Although not as obvious, the Fe emission features are also slightly smoothed. In the bottom panel, the effect on the P Cygni profile of He I λ3888 is clearly seen. Again, the change in the absorption component is obvious, but the effect on the emission is more difficult to see.

Lucy & Abbott (1993) found that such an extended acceleration could arise from changes in the ionization structure. A recent analysis of HD 50896 by Schmutz (1997) also suggests that the velocity law in that star is better characterized by a slow acceleration in the wind (i.e., a large β value). Observationally, it is very difficult to constrain the velocity law, particularly in WC stars. This difficulty arises from line blending and the influence of electron scattering and because most features are emitted from a region where the wind velocities are a substantial fraction (>60%) of the terminal velocity.

The extended acceleration zone has two major effects on the line profiles.[2] First, it produces broader and more extended P Cygni absorption in both resonance and subordinate lines. Second, unsaturated P Cygni absorption features are weaker (i.e., their minimum intensity is closer to the continuum level). This effect arises because the larger velocity gradient lowers the optical depth, particularly along sight lines that intersect the stellar core. The magnitude of both effects depends on the line under consideration. Examples of these effects are shown in Figure 11.

An additional benefit of the slower velocity law is that it smooths out the structure in the Fe V and Fe VI absorption/emission complexes shortward of 1500 Å and leads to a model spectrum more consistent with observation.

[2] Many of the C III lines are somewhat weaker in the model with the extended acceleration zone. However, the strength of the C III lines is not a diagnostic of the velocity law, since they are very dependent on the adopted stellar parameters.

12. RADIO FLUXES

Although our model does not extend into the radio region, it is possible to estimate the radio flux at 4.9 Ghz using the formulation of Wright & Barlow (1975). In the form given by Leitherer, Chapman, & Koribalski (1997), the radio flux is given by

$$S_\nu = 2.32 \times 10^4 \left(\frac{\dot{M} z}{v_\infty \mu}\right)^{4/3} \left(\frac{\gamma g_\nu \nu}{f d^3}\right)^{2/3} , \quad (9)$$

where μ is the mean ionic weight, γ is the mean number of electrons per ion, z is the root mean ionic charge, g_ν is the free-free Gaunt factor at frequency ν, and f is the filling factor. The dependence of S on f is from the work of Abbott et al. (1981).

At the outer boundary of our models, $r = 200R_*$, N_e is 10^8–10^9, depending on the model, and the dominant ionization states are He^+, C^{2+}, and O^{2+}. Assuming these values are reasonable for the radio-emitting region and using our model parameters of $\dot{M} = 1.5 \times 10^{-5}\ M_\odot\ yr^{-1}$, $V_\infty = 2300$ km s^{-1}, $d = 1.55$ kpc, C/He = 0.4, O/He = 0.1 (by number), and $f = 0.1$, we find

$$S_\nu(4.9\ \text{Ghz}) = 0.62\ \text{mJy} . \quad (10)$$

This exceeds the observed value of 0.33 ± 0.10 mJy by Abbott et al. (1982) by a factor of 1.9 and is larger than the formal errors.

There are several possible sources for the above discrepancy. First, to match the radio data we would need to reduce the mass-loss rate by a factor of 1.6. However, such a reduction would make the UV and optical fits unacceptable, even using a more peculiar reddening law.

Second, there could be variations in the filling factor between the radio and optical/UV line formation regions. For this effect to explain the discrepancy we would need the filling factor in the optical region to be 2.6 times smaller than that in the radio (i.e., the material in the radio region should be less clumped). Such a variation in filling factor is not unreasonable, but such a disparity between the filling factor in the radio and optical/UV line formation regions appears not to be required for O stars (e.g., Lamers & Leitherer 1993) or for WN7 stars for which radio observations are available (e.g., Crowther, Hillier, & Smith 1995a; but see the discussion by Hillier 1997).

A third possibility is that the ionization in the radio region is lower than assumed. If we fix all values in equation (9) and change only our assumptions about the ionization state in the radio region, we find the estimates listed in Table 2 for the 4.9 Ghz flux.

In Figures 12 and 13 we illustrate the UV energy and photon distributions shortward of 600 Å and mark the ionization energies of He^0, C^+, and O^+. The flux in this wave-

TABLE 2

PREDICTED 4.9 GHz RADIO FLUX AS A FUNCTION OF IONIZATION

Ionization State	Flux (mJy)
$He^+C^{2+}O^{2+}$	0.62
$He^+C^{2+}O^+$	0.56
$He^+C^+O^+$	0.36
$He^0C^+O^+$	0.08

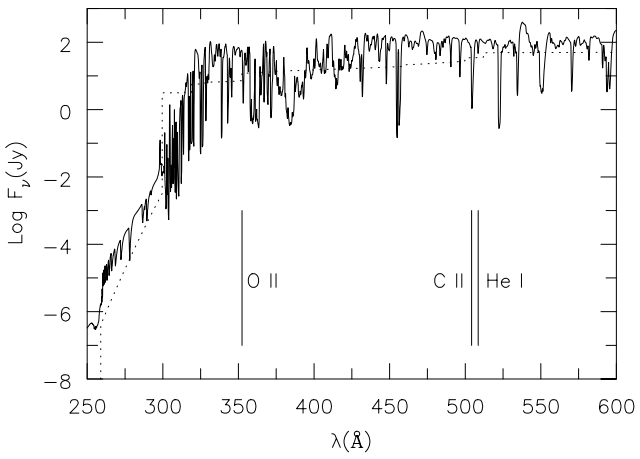

FIG. 12.—Theoretical energy distribution for HD 165763 shortward of the hydrogen Lyman limit. Several important ionization edges are also indicated. The blanketing shortward of 500 Å is expected to be even more severe when high iron levels and additional species are included. Also shown (*dotted line*) is the continuous energy distribution of the old model (Hillier 1989), which has been scaled by a factor of 1.35, so its fluxes match those of the present model at 6000 Å.

length range determines the ionization structure in the outer radio-emitting part of the atmosphere. It is quite possible that the flux shortward of the O II ionization edge could be reduced by the inclusion of nickel, cobalt, and higher levels in our iron atoms. This flux reduction might cause O^+ to be the dominant oxygen ionization stage in the radio-emitting region, but a reduction in the ionization states of C and He is much less likely. The conclusion is that the 4.9 Ghz fluxes in the top two rows of Figure 12 are reasonable for our models, but the bottom two rows are very unlikely. Thus it appears likely that ionization effects cannot explain the discrepancy between the observed and predicted radio fluxes.

In principal, we could use nebular analysis to place constraints on the ionizing flux. Rosa & Mathis (1990) concluded that the excitation of the nebula MR 26, whose central star is of type WC6, was so low that it was impossible to determine a reliable stellar temperature and nebular He abundance. The excitation they derived for the nebula is in fact lower than that for RCW 58, the nebula excited by the WN8 star HD 96548. More recent work by Esteben et al. (1992) showed that MR 26 is of low excitation with flux in the O II λλ3726, 3729 doublet over 6 times that in the O III λλ4959, 5007 doublet, but they noted that contamination by the Carina nebula is a severe problem and that the O II/O III flux ratio could be even larger. To help disentangle the nebular contribution, a comparison of O II images with O III images would be very beneficial, as would be velocity maps of the important diagnostic emission lines.

While MR26 (WC6) is of slightly lower excitation than HD 165763 (WC5), it does suggest that great care must be taken in deciding on the ionization balance when computing radio fluxes, a point previously made for WC stars by van der Hucht, Cassinelli, & Williams (1986). Given the problems with the ionization and filling factors, mass-loss rates derived from radio data may not be any more accurate than the mass-loss rates derived from direct modeling of WC spectra.

As a final source of error, we note that the predicted flux does depend on V_∞, d, and the composition. Errors due to V_∞ and composition should be small (i.e., $<20\%$); however, the error due to d could be substantial. In particular, if we adopted a normal reddening law, the models would require a distance of around 1.95 kpc, which reduces the predicted radio flux from 0.62 to 0.39 mJy, much closer to observation.

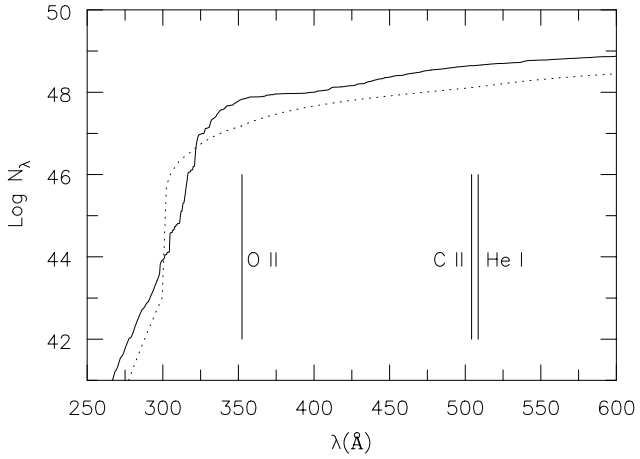

FIG. 13.—Plot showing log N_λ as a function of wavelength for the final model discussed in the text. The value N_λ is the total number of photons emitted with wavelength less than λ. The dotted line shows the cumulative photon distribution for the old model of Hillier (1989), which has been scaled by a factor of 1.35, so its fluxes match those of the present model at 6000 Å.

13. ABUNDANCES

13.1. C/He

The C/He abundance is moderately well determined ($0.2 < \mathrm{C/He} < 0.6$) and is primarily based on the He II λ5411/C IV λ5470 complex. The limits quoted are generous: 0.3–0.5 is probably a more realistic range. As has been noted by earlier studies, the ratio of these lines in the parameter domain of interest is insensitive to model details, and thus their ratio provides an excellent method for determining the C/He ratio. In addition, the He II and C IV atomic models are probably the most reliable. However, it should be stressed that it is important to have complete model atoms. When we increased the number of levels in our C IV atom from a maximum principal quantum number, n, of 16–30, we needed to reduce the C/He abundance ratio from 0.6 to 0.4 to produce a good fit to the carbon lines. Also, as noted by Bappu (1973), these lines are "relatively" blend-free, although in some of our models, particularly lower ionization models, the He II λ5411/C IV λ5470 features are affected by weak O III emission (see § 7 and Fig. 5).

In Figure 14 we illustrate the dependence of several lines on the C/He abundance ratio. Because of the high C mass fraction, He (e.g., He II λ5471 and He I λ10830) and O (see the oxygen complex from 3000 to 3500 Å) show a dependence on the C abundance. In the J band, not shown, there are two adjacent C/He line pairs whose ratios are also sensitive to the C/He abundance ratio.

Our final model has a carbon to helium number ratio of 0.4, which provides a very good fit to the He II λ5411/C IV λ5470 complex. Models with C/He less than 0.2 and higher than 1.0 are completely inconsistent with the observations

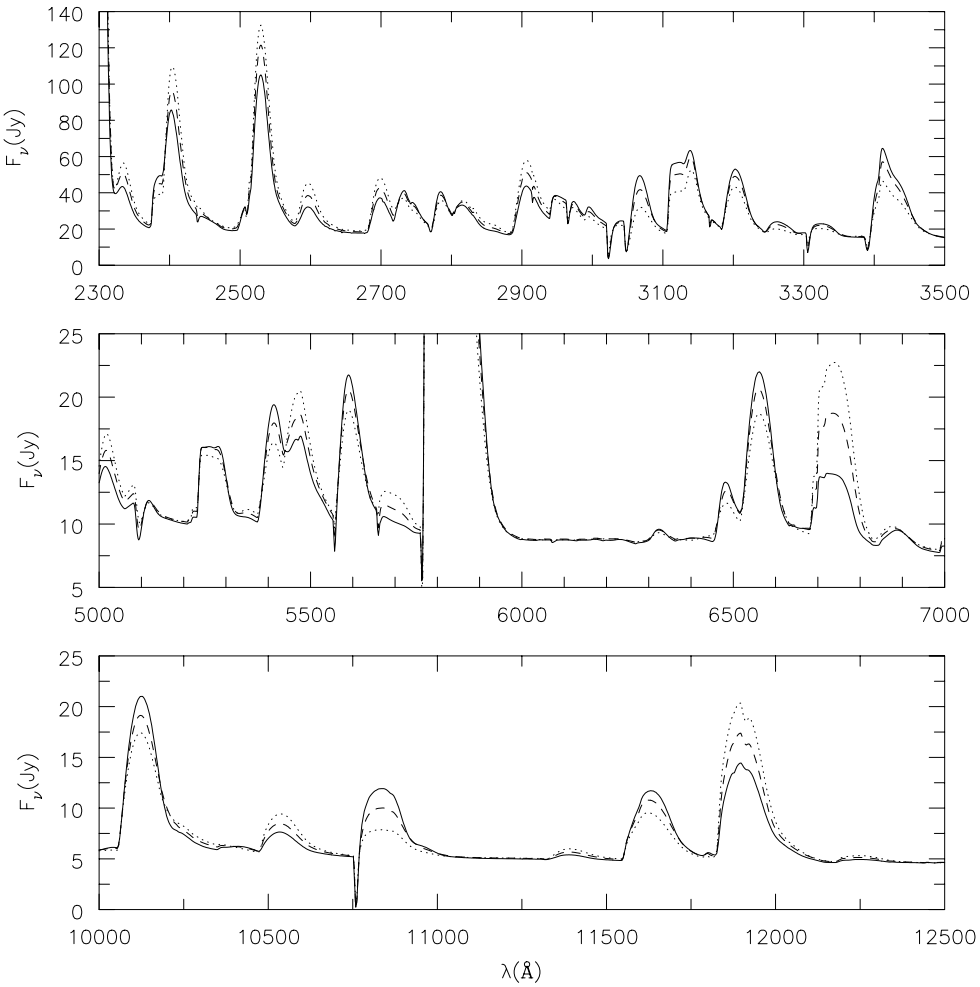

FIG. 14.—Illustration of the dependence of various lines on the C/He abundance ratio. Shown are theoretical spectra for C/He = 0.2 (*solid lines*), C/He = 0.4 (*dashed lines*), and C/He = 1.0 (*dotted lines*). All other parameters, including the O/He ratio, were held fixed. Notice the weakening of the oxygen lines between 3000 and 3500 Å as the carbon abundance increases. Also evident is the change in the relative strengths of He II λ5411 and C IV λ5471 lines.

and can be ruled out with very high confidence. Our value of 0.4 is in good agreement with earlier "recombination line" determinations of 0.2 by Nugis (1982), 0.5 by Hillier (1989), 0.33 by Koesterke & Hamann (1995), and 0.41 by Eenens & Williams (1992).

It is worth noting that clumping can indirectly influence the He II λ5411 to C IV λ5471 line ratio and thus the determination of the C/He ratio. This is because electron scattering moves photons from the line core into the wing of both lines, but those removed from He II λ5411 will blend in with C IV λ5471. Thus, in a homogeneous model, electron scattering preferentially removes electrons from the 5411 Å line. The effect of electron scattering on this blend is illustrated by Koesterke & Hamann (1995).

13.2. O/He *Abundance Ratio*

The O/He ratio is more problematic, and a quantitative assessment of the reliability of its determination is difficult, a fact already noted by Gräfner et al. (1998) in their study of LMC WC4 stars. Although O lines are prevalent in WC spectra, it is not easy to determine which features are best suited for quantitative analysis. First, not all lines show a strong sensitivity to the O abundance, but often their strength is primarily determined by the effective temperature. Second, lines of different ions can give results differing by as much as a factor of 2. This discrepancy could arise from error in the atomic data, the limited size of our atomic models or may reflect deficiencies in the atmospheric models. Third, the oxygen line strengths also respond to changes in the C/He abundance ratio.

The region from 3000 to 3500 Å is crucial for O abundance determinations: it contains lines due to O III, O IV, and O V (Fig. 15). In Figure 16 we illustrate the dependence of several O lines on the O/He abundance ratio. As apparent from this figure, O III λ3127 (M12), O IV λ3066 (M1), and O IV λ3409 (M2) are sensitive to the oxygen abundance and hence useful for O/He abundance ratio determinations. The O V λ5591 line is also sensitive to the oxygen abundance and is examined during the fitting procedure to find the best oxygen abundance.

Our best estimate of the O/He abundance is 0.1 by number, which fits most of the oxygen emission features to within a factor of 2. This value is somewhat of a compromise. With O/He = 0.05, the model matches many of the observed O III lines, but most other O lines are too weak. For O/He = 0.2, the O III lines are much too strong, as well as some of the O IV emission lines.

The most striking disagreement of the model with observation is for the O VI λλ3811, 3834 doublet, which is underestimated by a factor of 5. This discrepancy is most likely

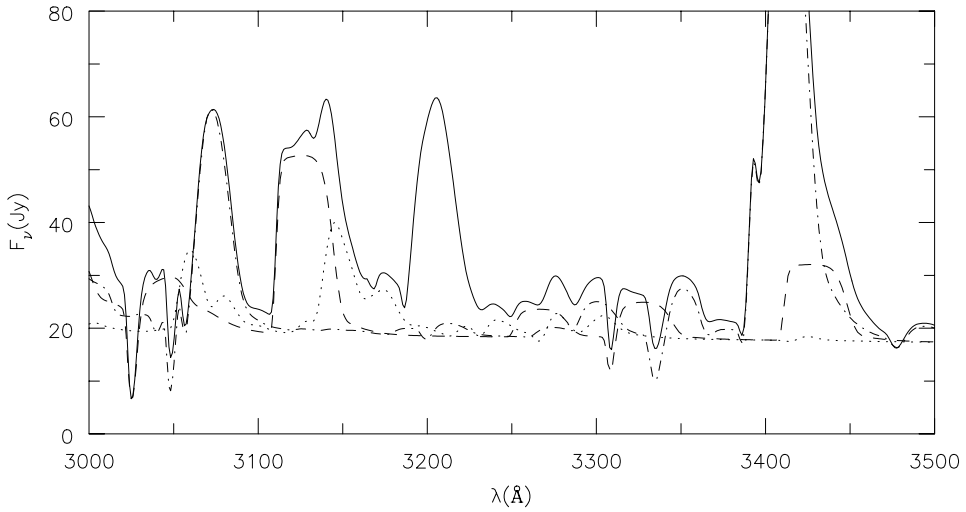

FIG. 15.—Illustration of the region from 3000 to 3500 Å for the final model showing the various O contributions. The solid line shows the spectrum when all species are included, and the dashed spectrum shows the contribution by O III, the dot-dashed spectrum shows that by O IV, and the dotted spectrum shows that by O V. The only strong feature not due to O in this region is located just longward of λ3200 and is a blend of He II and C IV.

due to a problem with the ionization structure and may be resolved when additional species are included. In a model with O/He = 0.1 with the luminosity increased by a factor of 1.5, the O V λ5591 line was in excellent agreement with observation, whereas the O VI doublet was now only a factor of 2 too weak.

As mentioned earlier, the atomic models are very important in spectroscopic analysis. Our early oxygen atomic models (see Table 1), particularly for the O III, O IV, and O V ions, are sufficient to survey parameter space but are much too incomplete for a detailed spectroscopic analysis. Even the model O ions in the final model, specifically O III, are too simple.

13.3. Fe *Abundance*

In stars with radiation driven winds, the metal abundance, Z, is crucial in determining the mass-loss rate. For O stars, calculations by Kudritzki, Pauldrach, & Puls (1987) and Kudritzki et al. (1991) suggest that the mass-loss scales as $Z^{0.5}$, although other calculations by Abbott (1982) and Shimada et al. (1994) indicate that the mass-loss rate scales as Z. For W-R stars the dependence is unknown but may be similar.

In order to place constraints on the iron abundance in HD 165763, we will examine theoretical spectra for the final model discussed in § 7, but for three different Fe mass fractions (0.25 solar, solar, and 4 solar, where the solar mass fraction is 1.5×10^{-3}; Gray 1992). The region most sensitive to the Fe abundance lies between 1350 and 1750 Å and is illustrated in Figure 17. Two effects are noticeable. First, variations in Fe abundance lead to a variation in the strength of the Fe emission features, thus allowing, in principal, the determination of the Fe abundance. Second, for the highest Fe abundance considered, the C IV λλ1548, 1551 emission doublet is almost completely eaten away by absorption. Comparison of the spectra with observation

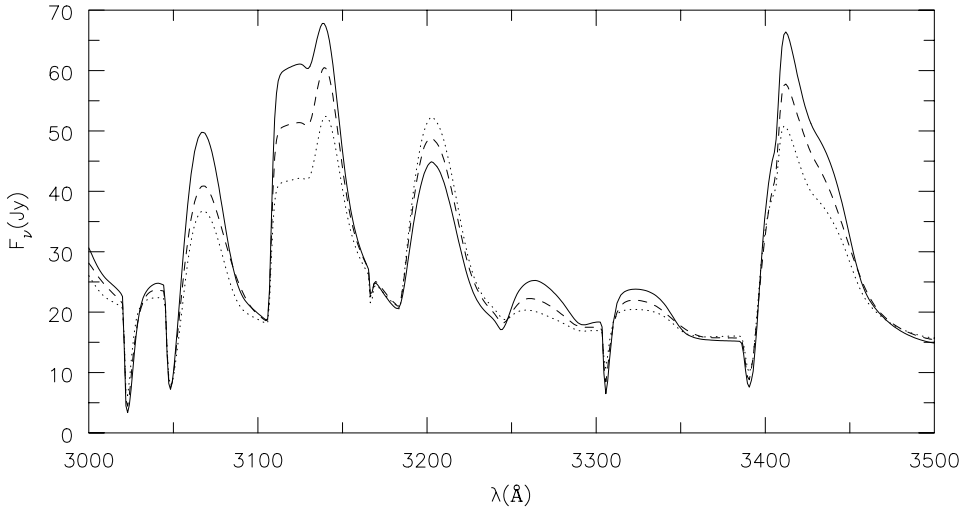

FIG. 16.—Illustration of the dependence of various lines on the O/He abundance ratio. Shown are theoretical spectra for O/He = 0.2 (*solid line*), O/He = 0.1 (*dashed line*), and O/He = 0.05 (*dotted line*). All other parameters, including the C/He ratio of 0.4, were held fixed. This spectral region is extremely important for determination of the O/He abundance ratio.

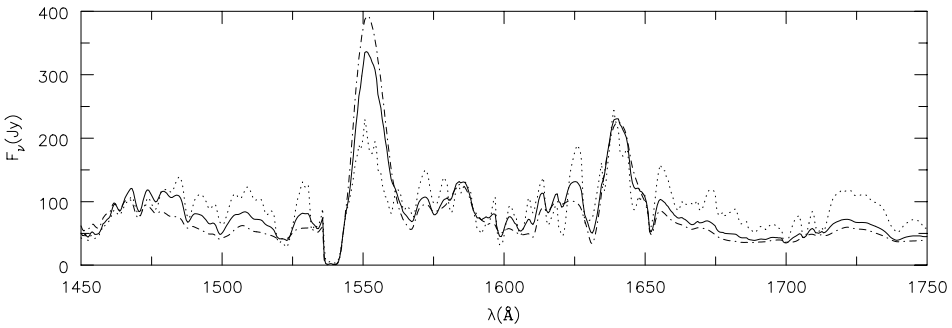

FIG. 17.—Comparison of theoretical spectra for three models of HD 165763 for Fe abundances of 0.25 solar (*dot-dashed line*), solar (*solid line*), and 4 solar (*dotted line*).

indicates that, although a solar metallicity does provide a reasonable fit to the Fe emission/absorption features, it is difficult to rule out Fe abundances up to a factor of 4 lower or up to a factor of 2 higher, especially considering systematic errors due to the adopted Fe model atoms and the neglect of other important blanketing species.

An examination of spectral regions longward of 1800 Å reveals that the spectrum is generally insensitive to the Fe abundance. Most lines vary at a level too small to affect the quality of the fits of the present analysis. However, some C III lines, C III λ5696 and C III λ2296, for example, show a significant variation with a change in iron abundance. The variation is not simply an ionization effect, for the magnitude and direction of the change depends on the C III line under consideration.

14. WIND MOMENTUM

One of the outstanding issues with W-R stars is what determines and what drives their large mass-loss rates. Although it is generally thought that radiation pressure is responsible, this process has difficulty explaining wind momentums that can exceed the radiation momentum by factors of 10–100 for WNE and WC stars. Whereas multiple scattering can in principal give the desired momentum deposition, it is unclear whether W-R stars have the necessary UV opacity for this to occur (e.g., Gayley et al. 1995). Since our model is lacking many high iron levels and important elements like nickel and cobalt, we cannot at present address this issue, but we are working toward remedying these deficiencies.

Although our results for HD 165763 reduce the momentum problem, they do not alleviate it completely. In the clumped model, the wind momentum to radiation momentum, $\dot{M}V_\infty/(L/c)$, is around 10, whereas the unclumped model has a ratio of 33. The ratio for our unclumped model is smaller than we found in previous studies because of the increase in the derived luminosity arising from the use of blanketed models. The clumped model has a further reduction because of its lower mass-loss rate.

The increasing observational (e.g., Robert 1994) and theoretical (Owocki et al. 1988; Owocki 1991) evidence for clumped winds in W-R stars and the ability of clumped models to match those observed (Hillier 1991b; Schmutz 1997; this paper) strongly suggest that clumped winds are the key to explaining the large "apparent" mass-loss rates of W-R stars. The filling factor approach we have used in this paper is relatively simple, and, given the broad lines and numerous blends, it is not possible to determine a reliable mass-loss rate and hence to determine how much the wind momentum actually exceeds the single scattering limit.

Such determinations, particularly for WC stars, might best be made observationally by analyzing eclipsing binaries (see St.-Louis et al. 1993; Lamontagne et al. 1996 for principles and application of this technique).

15. DISCUSSION

The improvement in our non-LTE model atmosphere code has allowed an improved spectroscopic analysis of the WC5 star HD 165763. The new calculations indicate a higher luminosity and a smaller core radius than that previously found, with both changes primarily attributed to the inclusion of line blanketing. The C/He abundance is similar to earlier determinations, but its value should be more reliable, because our calculations now include more accurate physics and better atomic data. An O/He abundance has also been deduced, but it is probably only accurate to a factor of 2. Our deduced C/He and C/O ratios of 0.4 and 4.0 are virtually identical to those derived for two Galactic and one LMC WO star by Kingsburgh, Barlow, & Storey (1994). This suggests that the difference between WO and WC stars is not due to O abundance but is more likely an excitation effect. The C/He and C/O ratios found for HD 165763 are also similar to the values found by Gräfner et al. (1998) for six LMC WC4 stars that had C/He = 0.2–0.5 and C/O = 1.8–6.7.

Our best models show excellent qualitative agreement with the observed spectrum of HD 165763 from the observable UV to the IR. Discrepancies between observations and spectra predicted using unblanketed models have been significantly reduced. At least some of the remaining discrepancies will be reduced as additional sources of line blanketing are included and as better atomic data becomes available. Some lines show unusual model dependencies, indicating that detailed blanketing calculations are necessary to model WC and probably WN spectra.

Despite the enormous advances in the last decade, the post–main-sequence evolution of massive stars in the H-R diagram is still very uncertain. Factors contributing to the uncertainties include mass-loss rates, the treatment of convection, the influence of stellar rotation, and the $C^{12}(\alpha, \gamma)O^{16}$ reaction rate. Maeder & Meynet (1994) show that the C/He and O/He abundances are sensitive to these effects and can thus provide important constraints on the evolution of massive stars.

Even though the abundances are uncertain, there is a well-defined mass-luminosity (M-L) relationship and a well-

defined R_*-M relationship (R_* is radius of hydrostatic evolution model), which are model-independent (Schaerer & Maeder 1992). Our derived radius of 1.8 $R_\odot$ for R_* is a factor of 2 larger than the model predictions (Table 3), but, given the uncertainties in the models and the difficulty in constraining R_*, the agreement is excellent. We predict, based on trends observed so far, that the inclusion of further blanketing effects in the atmospheric models will drive R_* toward the theoretical value for a standard $\beta = 1$ velocity law. This has obvious implications regarding how W-R winds are generated.

Maeder & Meynets (1994) have performed evolutionary calculations which track the surface C/He and O/He abundance ratios as a function of mass. Their high mass-loss rate calculations for $Z = 0.02$ indicate that a star with an initial mass of 60 $M_\odot$ and a current mass of 10 $M_\odot$ (as implied by our derived luminosity; see Table 3) will have a C/He abundance of 0.3 and an O/He abundance of 0.06. Such values are compatible with our derived values of 0.4 for the C/He ratio and 0.1 for the O/He ratio.

The O/He ratio at each epoch of a star's life is very sensitive to its mass at that epoch. For example, when a star with an initial zero-age main-sequence mass of 60 $M_\odot$ has a mass of $M = 12.6\ M_\odot$, the predicted O surface abundance is approximately 0.035, which is incompatible with our results. On the other hand, as the star's mass decreases with time, the O/He ratio increases to values well in excess of 0.1, in line with our predictions.

Clearly it is desirable that we perform the same analysis for other Galactic WC stars. This will allow both improved spectroscopic analysis, since discrepancies across WC subtypes can be better addressed and improved constraints on stellar evolution.

The power of using both the luminosity and abundances (O/He, C/He, and Fe/He) is that it allows the nondegenerate matching of observed stars to evolutionary tracks and thus can give both the initial and current masses. A discrepancy between just one of these four observed parameters would then indicate an inconsistency with the evolutionary models. The difficulty is to reduce the errors in the observed values for L, O/He, C/He, and Fe/H so that the comparisons are meaningful.

The quality of our fits together with earlier observational and theoretical evidence strongly suggests that W-R winds are clumped. If this is the case, mass-loss rates for W-R stars previously given in the literature need to be reduced by as much as a factor of 3. Such a reduction will strongly affect the theoretical evolution of W-R stars. Of course, a reduction in $\dot{M}$ through the W-R stage does not imply a similar reduction in earlier post–main-sequence phases. Mass loss in these stages, for example, the LBV stage, is also crucial to stellar evolution and affects the minimum C/He and O/He surface ratios in WC stars (Maeder & Meynet 1994).

Our new models demonstrate that spectroscopic analysis of WC stars requires accurate spectrophotometric data from UV to IR wavelengths. The difficulty of defining the continuum and correcting for line blends means that it is virtually impossible to determine reliable line profiles and EWs from observational data alone.

TABLE 3

PREDICTED EVOLUTIONARY MASS AND RADII AS A FUNCTION OF LUMINOSITY FROM SCHAERER & MAEDER (1992, EQS. [3] AND [4])

L ($L_\odot$)	M ($M_\odot$)	R_* ($R_\odot$)
1.0×10^5	7.2	0.69
2.0×10^5	10.5	0.86
3.0×10^5	13.3	0.98

The authors are indebted to the participants of the Opacity Project for supplying atomic data, without which these calculations would not be possible. We would especially like to thank Keith Butler, Anil Pradhan, Sultana Nahar, and Bob Kurucz for generously suppling atomic data, in some cases in advance of publication. This research was supported in part by NASA through grants 4450.01-92A and 5460.01-93A from the STScI, which is operated by AURA, Inc., under NASA contract NAS5-26555. Additional support was provided by NASA grant NAGW-3828.

REFERENCES

Abbott, D. C. 1982, ApJ, 259, 282
Abbott, D. C., Bieging, J. H., & Churchwell, E. 1981, ApJ, 250, 645
Auer, L. H., & Koenigsberger, G. 1994, ApJ, 436, 859
Bappu, M. K. V. 1973, in IAU Symp. 49, Wolf-Rayet and High Temperature Stars, ed. M. K. V. Bappu & J. Sahade (Boston: Reidel), 59
Becker, S. R., & Butler, K. 1995, A&A, 294, 215
Bieging, J. H., Abbott, D. C., & Churchwell, E. B. 1982, ApJ, 263, 207
Blomme, R., & Runacres, M. C. 1997, A&A, 323, 886
Cardelli, J. A., Clayton, G. C., & Mathis, J. S. 1988, ApJ, 329, L33
Clayton, G. C., & Mathis, J. S. 1988, ApJ, 327, 911
Cohen, M. 1995, ApJS, 100, 413
Cohen, M., Kuhi, L. V., & Barlow, M. J. 1975, A&A, 40, 291
Conti, P. S., Massey, P., & Vreux, J.-M. 1990, ApJ, 354, 359
Crowther, P. A, Hillier, D. J., & Smith, L. J. 1995a, A&A, 293, 403
Crowther, P. A, Smith, L. J., Hillier, D. J., & Schmutz, W. 1995b, A&A, 293, 427
Eaton, J. A., Cherepaschuk, A. M., & Khaliullin, Kh. F. 1985a, ApJ, 296, 222
———. 1985b, ApJ, 297, 266; erratum 334, 1076 (1988)
Eenens, P. R. J., & Williams, P. M. 1992, MNRAS, 255, 227
Eenens, P. R. J., Williams, P. M., & Wade, R. 1991, MNRAS, 252, 300
Esteban, C., Vilchez, J. M., Smith, L. J., & Clegg, R. E. S. 1992, A&A, 259, 629
Gayley, K. G., Owocki, S. P., & Cranmer, S. R. 1995, ApJ, 442, 296
Grafner, G., Hamann, W.-R., Hillier, D. J., & Koesterke, L. 1998, A&A, 329, 190
Gray, D. F. 1992, The Observation and Analysis of Stellar Photospheres (Cambridge: Cambridge Univ. Press)
Hamann, W.-R., Leunenhagen, U., Koesterke, L., & Wessolowski, U. 1992, A&A, 255, 200
Hillier, D. J. 1989, ApJ, 347, 392
———. 1991a, in IAU Symp. 143, Wolf-Rayet Stars and Interrelations with Other Massive Stars in Galaxies, ed. K. A. van der Hucht & B. Hidayat (Dordrecht: Kluwer), 59
———. 1991b, A&A, 247, 455
———. 1991c, in NATO ASI Ser. C, Vol. 341, Stellar Atmospheres: Beyond Classical Models (Dordrecht: Kluwer), 317
———. 1997, in Wolf-Rayet Stars in the Framework of Stellar Evolution, Proc. 33rd Liege International Astrophysical Colloquium, ed. J. M. Vreux, A. Detal, D. Fraipont-Caro, E. Gosset, & G. Rauw (Liége: Univ. Liége), 509
Hillier, D. J., & Miller, D. L. 1998, ApJ, 496, 407
Howarth, I. D., & Schmutz, W. 1992, A&A, 261, 503
Kingsburgh, R. L., Barlow, M. J., & Storey, P. J. 1994, A&A, 295, 75
Koenigsberger, G. 1990a, Rev. Mexicana Astron. Astrofis., 20, 85
———. 1990b, A&A, 235, 282
Koenigsberger, G., & Auer, L. H. 1985, ApJ, 297, 255
Koesterke, L., & Hamann, W.-R. 1995, A&A, 299, 503
Kudritzki, R. P., Pauldrach, A., & Puls, J. 1987, A&A, 173, 293
Kudritzki, R. P., Pauldrach, A., Puls, J., & Voels, S. R. 1991, in IAU Symp. 148, The Magellanic Clouds, ed. R. Haynes & D. Milne (Dordrecht: Kluwer), 279

Kuhi, L. 1968, in Wolf-Rayet Stars, ed. K. B. Gebbie & R. N. Thomas (National Bureau of Standards SP-307; Washington, DC: US GPO), 101
Kurosawa, R., Hillier, D. J., & Schulte-Ladbeck, R. E. 1999, AJ, in press
Kurucz, R. L. 1993, CD-ROM 22, Atomic Data for Fe and Na (Cambridge: Smithsonian Astrophys. Obs.)
Lamers, H. J. G. L. M., & Leitherer, C. 1993, ApJ, 412, 771
Lamers, H. J. G. L. M., & Waters, L. B. F. M. 1984, A&A, 138, 25
Lamontagne, R. 1983, Ph.D. thesis, Univ. Montréal
Lamontagne, R., Moffat, A. F. J., Drissen, L., Robert, C., & Mathews, J. M. 1996, AJ, 112, 2227
Leitherer, C., Chapman, J. M., & Koribalski, B. 1997, ApJ, 481, 898
Lucy, L. B., & Abbott, D. C. 1993, ApJ, 405, 738
Lundstrom, I., & Stenholm, B. 1984, A&AS, 58, 163
Maeder, A., & Meynet, G. 1994, A&A, 287, 803
Massey, P. 1984, ApJ, 281, 789
Meyer, D. M., & Savage, B. D. 1981, ApJ, 248, 545
Moffat, A. F. J. 1994, Ap&SS, 221, 467
Moffat, A. F. J., Owocki, S. P., Fullerton, A. W., & St-Louis, N., eds. 1994, Instability and Variability of Hot Star Winds, Ap&SS, 221, 1
Morris, P. W., Brownsberger, K. R., Conti, P. S., Massey, P., & Vacca, W. D. 1993, ApJ, 412, 324
Najarro, F., Hillier, D. J., & Stahl, O. 1997, A&A, 326, 1117
Nugis, T. 1982, in IAU Symp. 99, Wolf-Rayet Stars: Observations, Physics, Evolution, ed. C. W. H. De Loore & A. J. Willis (Dordrecht: Reidel), 127
———. 1994, Ap&SS, 221, 217
Nugis, T., & Sapar, A. 1985, Tartu Astrofuus. Obs. Teated, 80
Nussbaumer, H., Schmutz, W., Smith, L. J., & Willis, A. J. 1982, A&A, 47, 257
Owocki, S. P., Castor, J. I., & Rybicki, G. B. 1988, ApJ, 335, 914
Owocki, S. P. 1991, in NATO ASI Ser. C, Vol. 341, Stellar Atmospheres: Beyond Classical Models (Dordrecht: Kluwer), 235
Puls, J., Owocki, S. P., & Fullerton, A. W. 1993, A&A, 279, 457
Robert, C. 1994, A&SS, 221, 137
Rosa, M. R., & Mathis, J. S. 1990, in ASP Conf. Ser. 7, Properties of Hot Luminous Stars, ed. C. D. Garmany (San Francisco: ASP), 135
Schaerer, D., & Maeder A. 1992, A&A, 263, 129
Schulte-Ladbeck, R. L., Eenens, P. R. J., & Davis, K. 1995, ApJ, 454, 917
Seaton, M. J. 1979, MNRAS, 187, 73P
———. 1987, J. Phys. B, 20, 6363
Serkowski, K., Mathewson, D. S, & Ford, V. L. 1975, AJ, 196, 261
Schmutz, W. 1997, A&A, 321, 268
Schmutz, W., Hamann, W.-R., & Wessolowski, U. 1989, A&A, 210, 236
Shimada, M. R., Ito, M., Hirata, R., & Horaguchi, T. 1994, in IAU Symp. 162, Pulsation, Rotation and Mass Loss in Early-Type Stars, ed. L. A. Balona, H. F. Henrichs, & J. M. Le Contel (Dordrecht: Kluwer), 487
Springmann, U. 1994, A&A, 289, 505
St.-Louis, N., Drissen, L., Moffat, A. F. J., Bastien, P., & Tapia, S. 1987, ApJ, 322, 870
St.-Louis, N., Moffat, A. F. J., Lapointe, L., Efimov, Y. S., Shakhovskoy, N. M., Fox, G. K., & Pirola, V. 1993, ApJ, 410, 342
Torres, A. V., Conti, P. S., & Massey, P. 1986, ApJ, 300, 379
van der Hucht, K. A., Cassinelli, J. P., & Williams, P. M. 1986, A&A, 168, 11
Vreux, J.-M., Andrillat, Y., & Biemont, E. 1990, A&A, 238, 207
Wright, A. E., & Barlow, M. J. 1975, MNRAS, 170, 41